Urban Forestry & Urban Greening 78 (2022) 127783

Contents lists available at ScienceDirect

Urban Forestry & Urban Greening

journal homepage: www.elsevier.com/locate/ufug

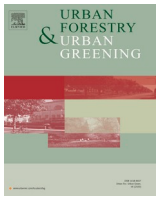

Original article

Detection of unfavourable urban areas with higher temperatures and lack of green spaces using satellite imagery in sixteen Spanish cities

Francisco Rodríguez-Gómez [a], Rafael Fernández-Cañero [b], Gabriel Pérez [c], José del Campo-Ávila [a], Domingo López-Rodríguez [d], Luis Pérez-Urrestarazu [e,*]

[a] Departamento de Lenguajes y Ciencias de la Computación, Universidad de Málaga, Campus de Teatinos, 29071 Malaga, Spain
[b] Urban Greening & Biosystems Engineering Research Group, Department of Agronomy, Universidad de Sevilla, ETSIA, Ctra. Utrera km.1, 41013 Seville, Spain
[c] Department of Computer Science and Industrial Engineering, Universitat de Lleida, C/Jaume II 69, Lleida 25001, Spain
[d] Universidad de Málaga, Departamento de Matemática Aplicada, Campus de Teatinos, 29071 Málaga, Spain
[e] Urban Greening & Biosystems Engineering Research Group, Area of Agro-Forestry Engineering, Universidad de Sevilla, ETSIA, Ctra. Utrera km.1, 41013 Seville, Spain

ARTICLE INFO

Handling Editor: Dr Cecil Konijnendijk van den Bosch

Keywords:
Urban greening
Remote sensing
Heat island
Normalized difference vegetation index
Landsat-8

ABSTRACT

This paper seeks to identify the most unfavourable areas of a city in terms of high temperatures and the absence of green infrastructure. An automatic methodology based on remote sensing and data analysis has been developed and applied in sixteen Spanish cities with different characteristics. Landsat-8 satellite images were selected for each city from the July-August period of 2019 and 2020 to calculate the spatial variation of land surface temperature (LST). The Normalized Difference Vegetation Index (NDVI) was used to determine the abundance of vegetation across the city. Based on the NDVI and LST maps created, a k-means unsupervised classification clustering was performed to automatically identify the different clusters according to how favourable these areas were in terms of temperature and presence of vegetation. A Disadvantaged Area Index (DAI), combining both variables, was developed to produce a map showing the most unfavourable areas for each city. Overall, the percentage of the area susceptible to improvement with more vegetation in the cities studied ranged from 13 % in Huesca to 64–65 % in Bilbao and Valencia. The influence of several factors, such as the presence of water bodies or large buildings, is discussed. Detecting unfavourable areas is a very interesting tool for defining future planning strategy for green spaces.

1. Introduction

Urban areas face serious challenges due to rapid urbanization and population growth in cities. Global warming and urbanization can increase temperatures in and around cities, exacerbating the Urban Heat Island Effect (UHI), especially during heat waves (Santamouris, 2013). The UHI is a climatic phenomenon consisting of higher urban temperatures developing in an urban area, compared to the surrounding suburban and rural areas. This has a significant impact on energy consumption and the urban environment (Santamouris et al., 2007). It is the most documented climate change phenomenon and has been studied in detail in numerous cities worldwide (Imhoff et al., 2010; Theeuwes et al., 2017; Tran et al., 2006).

The UHI is related to the positive heat balance created in the urban environment as the heat generated there (due to the high absorption of solar radiation and anthropogenic heat) is trapped in urban structures. This situation is exacerbated by greenhouse gases and the lack of green spaces (Susca et al., 2011). In this regard, numerous scientists propose increasing urban vegetation as a possible UHI mitigation strategy, since numerous studies have established the correlation between an increase in green areas and a reduction in local temperature (Qiu et al., 2013; Susca et al., 2011; Takebayashi and Moriyama, 2007).

An important mechanism for cities to adapt and improve their resilience is to redesign their infrastructures and increase the role of the urban green infrastructure (UGI). The UGI includes public parks, nature reserves, forests, streams, greenways and walkways, community gardens, rain gardens, and green roofs (Wolch et al., 2014). In fact, any outdoor space that is partially or entirely covered with vegetation such as grass, shrubs, trees, or other types of vegetation is considered to make up the UGI (Environmental Protection Agency, 2014).

The UGI is an important feature of cities that provides critical ecosystem services such as mitigating global warming and reducing

* Corresponding author.
E-mail address: lperez@us.es (L. Pérez-Urrestarazu).

https://doi.org/10.1016/j.ufug.2022.127783
Received 30 April 2022; Received in revised form 27 October 2022; Accepted 1 November 2022
Available online 5 November 2022

atmospheric pollution (Gupta et al., 2012; Liu and Russo, 2021). Furthermore, the UGI benefits include the provision of environmental requirements, such as fresh water (Yang et al., 2015), food production (Grafius et al., 2020), recreation and aesthetic pleasure (Grunewald et al., 2017; Wang et al., 2019). Additionally, although often overlooked, the UGI can make a major contribution to the economic and social development of cities (Levent and Nijkamp, 2017) and increase the quality of life of their citizens (Giannico et al., 2021).

The use of satellite imagery to study climatic phenomena or UGI distributions on a city scale is very helpful. According to Shahtahmassebi et al. (2021) the number of studies focusing on mapping has increased rapidly over the last decade. Remote sensing technologies can provide repeated and complete coverage at different spatial scales and seasons. They minimize the need for field survey, as high spatial resolution imagery and free data access policies make remote sensing a valuable tool (Zhu et al., 2019), even in highly heterogeneous and complex urban settings. Programmes such as Copernicus (European Commission, 2014) and Landsat (NASA, 1972) provide both historical time-series and recently acquired data.

Different analytical techniques can be used in the remote sensing of the UGI, such as object-based image analysis or land cover indices. They typically use combinations of different wave bands from multispectral satellite sensors. The Normalized Difference Vegetation Index (NDVI) is the best-known and most widely applied index for mapping the UGI (Xue and Su, 2017), among land cover indices, and useful to differentiate green and non-green regions within urban areas.

Although traditional methods for measuring air temperature at meteorological stations offer the advantage of obtaining accurate data, the density of the meteorological station distribution is limited, leading to poor coverage. On the contrary, the remote sensing method achieves excellent synchronicity and spatial coverage, which overcomes the weakness of the traditional method (Du et al., 2017).

Remotely sensed thermal infrared imagery retrieved from satellites can be used to calculate the land surface temperature (LST), which is regarded as an indicator of the air temperature close to the surface (Schwarz et al., 2012; Voogt and Oke, 2003). In fact, Herrera-Gomez et al. (2017) observed a high correlation between the LST obtained by Landsat 7 images and ambient temperature data retrieved from weather stations located at different sites in Seville (Spain).

Estoque et al. (2017) found a significantly strong correlation between mean LST and the density of impervious surface (positive) and green space (negative) along the urban-rural gradients of the cities studied, depicting a typical UHI profile. Their study sought to examine the relationship between land surface temperature (LST) and the abundance and spatial pattern of impervious surface and green space in three metropolitan areas using Landsat-8 OLI/TIRS data. On average, the mean LST of the impervious surfaces was around 3 °C higher than that of the green space. Other authors also reported the inverse relationship between NDVI (as a measure of the abundance of vegetation) and LST (Herrera-Gomez et al., 2017; Huang and Ye, 2015; Susca et al., 2011; Yue et al., 2007). The strength of the correlations depends on the season, time of day, and land cover (Marzban et al., 2018). Furthermore, the characteristics, abundance and spatial distribution of the UGI influence the effectiveness in mitigating the UHI (Park et al., 2017; Yang et al., 2017), which makes the characterization of existing green areas in a city important.

In this context, different studies in recent years have assessed the role that vegetation plays in the decrease in temperatures in urban environments. Although some rely on remote sensing (e.g., Du et al., 2017; Estoque et al., 2017; Reis and Lopes, 2019), the data acquisition and result process was not automated. Furthermore, as the urban space and resources to create new UGI are limited, determining the most unfavourable areas of a city in terms of high temperatures and the absence of UGI is essential and constitutes the main objective of this paper. The main innovations presented are (1) the identification of those unfavourable zones and (2) the automation of the process.

Therefore, in order to meet these two challenges, a new methodology for the automatic retrieval of information at municipality level from satellite images has been applied to sixteen Spanish cities with different characteristics in order to verify its feasibility and applicability. In them, urban areas were evaluated in terms of their temperatures and the presence of vegetation. The most unfavourable locations in each of the cities studied were identified using that information.

2. Methods

2.1. Description of the cities studied and selection criteria

Sixteen Spanish cities were selected for the study (Table 1) in order to cover several locations of Spanish geography with different climates, including cities of various sizes and quantity of UGI. According to their climatic characteristics, they were categorised into four groups: (I) inland cities with hot summers, (II) Mediterranean cities with coast, (III) northern cities close to the sea, and (IV) northern cities far from the sea. Cities in groups I and II are characterised by a prolonged warm period during spring and summer, though the former reaches very high temperatures. In contrast, milder ones, with a higher relative humidity, are observed in the latter. Cities in group III have lower temperatures in summer. Cities in group IV also present lower temperatures than those in the south, although they can reach high temperatures (over 30º) at specific time periods.

2.2. Data retrieval process

Four or five Landsat-8 satellite images (depending on their availability) were downloaded from Earth Explorer (USGS, Department of the Interior, United States, http://earthexplorer.usgs.gov) for each of the cities. They were selected in the July-August period of 2019 and 2020, from among those with less than 5 % cloud cover that showed temperatures closer to the average of the month in each city. The dates of the images selected in the different cities studied were not the same, and heatwaves were avoided in order to prevent unreliable results. The images, with a pixel size of 30 m x 30 m, were cropped to fit the area of interest and the desired UTM coordinates introduced. After being processed, some of the images had to be discarded due to corrupted data or missing information. However, at least three images per city were finally used.

Additional images in autumn, winter, and spring were selected for two cities (Malaga and Seville), in order to assess the methodology (and detect discrepancies) not only in the most unfavourable dates, but all over a complete year.

The data on the green infrastructure and the observed temperatures was retrieved and computed from the images of each city using the R programming language (R Core Team, 2021). The R libraries used were raster, dplyr, rgdal, factoextra, NBClust, sp, and ggplot2, inter alia. Therefore, the spatial distribution of these two variables was obtained.

2.3. Vegetated areas detection and classification

The Normalized Difference Vegetation Index (NDVI) was used to identify the areas covered by vegetation and its amount. The NDVI is a numerical index that indicates the presence or absence of vegetation, as its value depends on the amount and physiological state of the plant cover (Liao et al., 2005; Tan et al., 2010). It varies from 0.0 to 1.0, with water being below 0 (Chen et al., 2006; Small, 2010).

The NDVI value for each pixel of the areas of interest in all cities was calculated as follows (Taufik et al., 2016):

$$NDVI = (b5-b4)\,(b5+b4)^{-1} \quad (1)$$

where b5 is the near-infrared band and b4, the red band.

There are different classifications according to the NDVI values in

Table 1
Selected cities and their characteristics: Inhabitants, size of the urban area studied, green areas (surface and area per inhabitant) (Holidu, 2019), climatic area according to the Spanish Technical Building Code ("Código Técnico de la Edificación", 2020) and average temperature in summer (AEMET, n.d.).

Group	City	Inhabitants	Urban Area (Km^2)	Green areas per inhabitant[a] (m^2/inhab)	Climatic area[b]	Average temp.[c] (ºC)
I	Madrid	3183 K	274	15.78	C	26.9
	Seville	689 K	75	11.27	B	28.6
	Murcia	443 K	9.7	3.38	B	26.6
	Ciudad Real	75 K	9	31.44	C	27.8
	Alcobendas	116 K	18.7	15.13	C	26.7
II	Barcelona	1621 K	76.8	5.53	C	24.3
	Valencia	788 K	73	4.19	B	26.8
	Malaga	569 K	93.3	2.92	A	27.3
	Palma de Mallorca	416 K	27.7	3.34	B	26.2
III	Bilbao	345 K	17.5	5.74	C	21.6
	Vigo	293 K	5.9	3.65	C	20.5
	Vitoria	247 K	28.7	26.76	D	19.4
	Santiago de Compostela	96 K	10.1	23.61	C	18.7
IV	Zaragoza	665 K	47.6	9.02	C	26.7
	Huesca	220 K	2.9	5.69	C	25.1
	Lleida	138 K	10.2	10.13	C	25.8

[a] To calculate the ratio of green areas per inhabitant, data were extracted from OpenStreetMap (OSM), considering the parks in each city labelled as "leisure=park" (Holidu, 2019)
[b] Classification according to the Spanish Technical Building Code ("Código Técnico de la Edificación", 2020)
[c] Calculated as the mean of average temperatures in July and August in 2019 and 2020 for each city

terms of vegetation abundance. For example, Taufik et al. (2016) made three categories: water (NDVI<0.1), non-vegetation (0.2–0.5) and vegetation (0.6–0.9). Farina (2012) determined for Seville (one of the cities used in our study) that pixels with positive NDVI values lower than 0.2 included man-made materials with no or sparse vegetation. NDVI values higher than 0.5 were considered fully vegetated, while NDVI values between 0.2 and 0.5 corresponded to a mixture of man-made materials and vegetation. Similarly, Hashim et al. (2019) established the following categories: non-vegetation (<0.2), low vegetation (0.2–0.5), and high vegetation (>0.5). For our study, an intermediate category corresponding to moderate vegetation was included according to Fusami et al. (2020). Therefore, values obtained were classified as water (NDVI < 0), no vegetation (0 < NDVI ≤ 0.2), low vegetation (0.2 < NDVI ≤ 0.4), moderate vegetation (0.4 < NDVI ≤ 0.6) and dense vegetation (0.6 < NDVI ≤ 1).

Finally, in order to validate the results obtained with this procedure, the vegetation maps generated in two cities (Malaga and Seville) were compared with the maps of Land Cover/Use classes established in the Urban Atlas Copernicus project (https://land.copernicus.eu/local/urban-atlas). For that, the Urban Atlas 2018 maps for these cities were

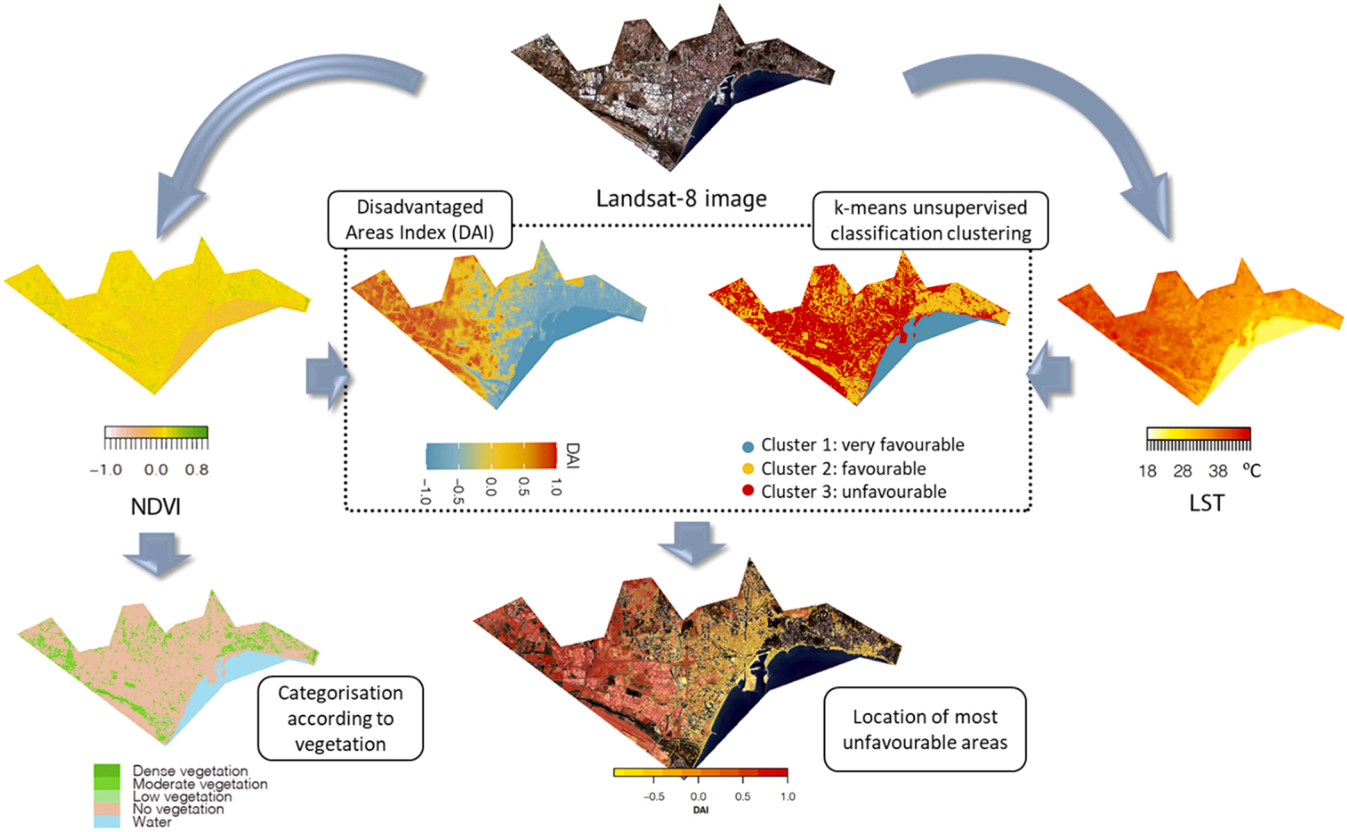

Fig. 1. Process for determining the most unfavourable areas.

downloaded and the layers corresponding to the following land uses (compatible with the inclusion of vegetation) were isolated: Green urban areas (14100), Forests (31000), Herbaceous vegetation associations (32000), Permanent crops (22000), and Pastures (23000). Lastly, a map overlapping the information of both vegetation (derived from NDVI values classification) and land uses (from Urban Atlas) was created to show the degree of coincidence. It should be noted that this last step was manually performed and was not part of the automated methodology.

2.4. Temperature calculation

A Raster map with the LST was created for each Landsat image of the different cities. The Landsat-8 OLI (Operational Land Imager) and TIRS (Thermal Infrared Sensor) Landsat-8 band data was therefore converted to Top of Atmospheric (TOA) spectral radiance using the rescaling factors provided in the metadata file. The TOA spectral radiance was then converted to brightness temperature to obtain LST following the procedure described by Mejbel Salih et al. (2018). The Land Surface Emissivity (computed from NDVI values) was also used.

2.5. Determination of the most unfavourable areas

Fig. 1 shows the complete process with the different steps performed The LST and NDVI maps obtained for each city were used to generate a further two maps prior to determine the most unfavourable areas in terms of the lower amount of vegetation present and higher temperatures.

An indicator was developed for the first to quantify the 'degree of disadvantage' of each region. Therefore, the Disadvantaged Area Index (DAI) was again calculated for each pixel as follows:

$$DAI_i = \left(1 - \frac{\tanh(NDVI_i)}{\tanh(1)}\right) \cdot \tanh\left(\frac{LST_i - LST_{av}}{LST_{sd}}\right) \quad (2)$$

where:

DAI_i is the Disadvantaged Area Index for pixel i.

$NDVI_i$ is the Normalized Difference Vegetation Index of pixel i.

LST_i is the Land Surface Temperature of pixel i.

LST_{av} is the average value of the Land Surface Temperature of every pixel in the image.

LST_{sd} is the standard deviation of the Land Surface Temperature values of every pixel in the image.

The LST of pixels with NDVI < 0 (water) was not considered to calculate LST_{av} and LST_{sd}.

This index is intended to give low ratings to locations with more vegetation (high NDVI) and cooler temperatures than other areas. High DAI values are obtained when higher temperatures are observed in a location with little or no vegetation. The hyperbolic tangent function assures that the DAI value for nonnegative NDVI values is between -1 and 1. The sign of the DAI in a given pixel will correspond to the temperature in that pixel in relation to the region's mean temperature.

Based on the NDVI and LST maps, a k-means unsupervised classification clustering was likewise performed to automatically identify the different clusters according to how favourable these areas were in terms of temperature and presence of UGI. For this methodology, the number of clusters must be decided a priori and three clusters were therefore set. One out of those three clusters grouped the most unfavourable areas, another the most favourable, and the last was for intermediate zones.

Although both methods (DAI and k-means) use information about vegetation (NDVI) and temperature (LST), the former combines information using an ad hoc index designed by experts, and the latter discovers relationships between similar points without any prior knowledge of the experts (non-supervised method).

Once the clustering process determines the different regions that share common characteristics, those regions need a semantic labelling (more favourable areas, favourable areas and unfavourable areas). Such labelling is given using DAI information.

To finally determine the most disadvantaged areas, the DAI and clustering information are combined. First, only points determined within the cluster labelled as unfavourable are considered. Then for those points, the DAI value is used. That is, if a point is not included in an unfavourable area, it is filtered and not considered because it is not relevant to identify unfavourable points. These DAI values calculated for the pixels in the most unfavourable cluster were presented in a final map. A kmz file was created for each city and imported to Google Earth Pro 7.3.4., so the DAI map over layed an aerial image.

3. Results

The LST and NDVI maps obtained for the studied cities are shown in the Supplementary Information (Appendix A). Only one map per city (both for LST and NDVI) is presented as an example. Each of them is accompanied by a histogram showing the distribution of values.

In addition, a map per city was created showing the distribution of zones in each category (moderate, low, or no vegetation and water) (Appendix A). Furthermore, Table 2 shows the surface and percentage of the total area of the city in each of the said categories and those corresponding to the areas determined as the most unfavourable. The area corresponding to dense vegetation was negligible, so it was not considered.

Fig. 2 shows maps with the most unfavourable areas in each city overlapped with an aerial view (the maps are presented in greater detail in Appendix B). The DAI value within those areas is indicated using a colour code, with red zones corresponding to a higher DAI.

4. Discussion

Overall, the percentage of the area susceptible to improvement with more vegetation in the cities studied changed substantially from one city to another. For example, only 13 % of Huesca's total area was identified as unfavourable, while Bilbao and Valencia are well over 60 %.

It should be noted that having a larger unfavourable surface area (or a higher proportion of the city catalogued as such) does not mean that the city has fewer UGIs or a worse heat problem compared to another with less unfavourable areas. This happens because both DAI and k-means clustering are based on the complete dataset of that particular city, which is somehow 'normalised'. Therefore, cities such as Santiago de Compostela, with a high amount of UGIs and not many areas with extreme temperatures, show a higher percentage of unfavourable areas than other such as Ciudad Real. Hence, this methodology is not meant to be a comparison between cities, but a tool to decide the best location for the UGI within each urban area. In any case, the NDVI histograms presented in Appendix A for each city are a good indicator of the abundance of vegetation in them and could be used to compare cities or determine which one is in more need of introducing green infrastructure.

In terms of deciding where to locate the new UGI, and given that the cooling effects of green areas can be observed within a maximum distance between 35 and 840 m (Lin et al., 2015), it is important to consider the landscape connectivity because it can modify the effects of green areas on variations in LST (Sun et al., 2018). This fact can be observed, for instance, in Alcobendas, where the south-east of the city has very high UGI coverage with good connectivity, which produces a cooling effect with differences of even 10ºC compared to the other areas of the city (Appendix A). Vitoria and Santiago de Compostela are also examples of good UGI connectivity. The same was observed by Masoudi and Tan (2019) in Singapore and Chen et al. (2014) in Beijing, where they found an important effect of the spatial pattern (size, shape complexity, fragmentation, and connectivity of the UGI).

In many areas identified as unfavourable, there is no space available for including parks, gardens, or even trees. In those cases, the role of building-integrated vegetation (i.e., green roofs and vertical greening systems) to increase green areas and ensure connectivity is fundamental

Table 2
Surface and proportion over the total area in the different categories: Moderate vegetation, low vegetation, no vegetation, water, unfavourable areas.

Group	City	Surface (km^2)					proportion over the total area (%)				unfavourable area	
		water	no vegetation	low vegetation	moderate vegetation	total	water	no vegetation	low vegetation	moderate vegetation	Surface (km^2)	Proportion (%)
I	Madrid	0.7	199	69.3	5	274	0.2	72.6	25.3	1.8	80.7	29.4
	Seville	1.4	60.5	12.4	0.7	75	1.8	80.7	16.5	1	25.8	34.3
	Murcia	0.1	7.8	1.7	0	9.7	0.7	81.1	17.8	0.4	3.1	32.5
	Ciudad Real	0	7.3	1.5	0	9	0.5	81.8	17.3	0.4	2.5	27.9
	Alcobendas	0.1	9	8.8	0.8	18.7	0.5	48.2	47	4.3	7.4	39.4
II	Barcelona	0.3	66.3	10.2	0	76.8	0.4	86.3	13.3	0	41.3	53.8
	Valencia	11.3	52.6	8.5	0.6	73	15.4	72.1	11.6	0.8	47.8	65.4
	Malaga	11.3	71.2	10.5	0.3	93.3	12.1	76.3	11.3	0.3	52.3	56.1
	Palma de Mallorca	0	20	7	0.7	27.7	0.2	72.2	25.1	2.6	14.1	50.8
III	Bilbao	0.7	11.3	3.9	1.6	17.5	3.8	64.7	22.1	9.3	11.2	64.1
	Vigo	0	4.5	1.3	0.1	5.9	0.2	76.1	21.9	1.8	3.5	58.2
	Vitoria	0.4	17.8	8.6	2	28.7	1.3	61.9	30	6.9	7.6	26.3
	Santiago de Compostela	0	4.3	3.9	1.9	10.1	0.1	42.8	38.6	18.3	4.2	42
IV	Zaragoza	0.6	34.8	11.5	0.6	47.6	1.3	73.1	24.2	1.3	19.8	41.7
	Huesca	0	2.4	0.5	0	2.9	0	80.5	18.7	0.7	0.4	13
	Lleida	0	6.7	2.8	0.7	10.2	0.4	65.9	27.3	6.4	6.1	59.6

(Herrera-Gomez et al., 2017).

Not only does UGI affect the temperature in a particular area of the city, but also other factors come into play. The influence of the presence of water bodies is evident (Cai et al., 2018; Li et al., 2022). Unfavourable areas tend to be far from the coastline in Malaga, Palma de Mallorca and Barcelona, but, curiously, not in Valencia (where vast impervious, non-vegetated zones are observed near the sea). The influence of the UGI on the LST likewise tends to be higher far from the coast than near it (Ossola et al., 2021).

Dynamic blue spaces such as rivers can absorb radiation by advection and release energy out of the urban system (Hathway and Sharples, 2012). For example, the most unfavourable areas are not close to the River Guadalquivir in Seville or the River Ebro in Zaragoza. Exceptions to this can be seen, for example, in Lleida. Although the favourable effect on the urban temperatures provided by the river crossing the city and the large riverside forest located in the north-east sector of the city is perfectly observed, some very unfavourable areas are encountered near the river and the riverside forest. These areas correspond mainly to two urban typologies: (a) zones with large, paved surfaces (e.g., large squares, supermarket parking lots, school yards, etc) and (b) groups of large industrial buildings with metal or gravel-ballasted roofs, that are flat or slightly sloped. As shown in Fig. 3, neither the river nor the river forest can compensate for this negative effect on urban temperatures. Therefore, more trees should be planted on large paved plots and industrial buildings should be encouraged to integrate green roofs or vertical greening systems. This is also applicable to large buildings in the city centre, such as train stations (e.g., Atocha Station in Madrid or Santa Justa Station in Seville).

Industrial areas are usually included in the group of most disadvantaged zones in all the cities studied, as they are formed by large buildings constructed with materials that accumulate heat and surrounded by impervious areas with very little vegetation. For example, the few unfavourable areas encountered in Vitoria and Huesca precisely have those characteristics, in contrast to the rest of the city where the UGI configuration is very spread and connected (Fig. 4).

In some cases, the unfavourable zones are not in the city centre but in the outskirts where there are bare areas without buildings or vegetation. They usually have dark, dry soils that accumulate more temperature. This happens, for instance, in some areas of Madrid, Ciudad Real or Malaga. These bare areas present an enormous opportunity to create green belts around the cities. In these cases, the type (and colour) of the surface clearly affects their temperature (Aletba et al., 2021). As another example, one of the areas with a higher DAI value in Valencia comprises several sports courts (none of which have natural grass).

Not only is the location of the UGI important, but there are also other variables to be considered. The type of vegetation used and the density are key factors affecting the effectiveness of reducing urban temperature. Different cooling benefits are generated the different urban vegetation types as in each of them a certain effect prevails (e.g., cooling by evapotranspiration, shading) (Su et al., 2022). For example, a study carried out in 293 European cities (Schwaab et al., 2021) showed that urban trees were related to reductions in LST 2–4 times higher than the reduction in LST associated with treeless UGI. Differences in LST of 1.6 ºC on average were observed between trees and lawns, especially on the days with insufficient water supply Liu et al. (2022) and Li et al. (2022) reported a cooling effect of dense trees ranging from − 6.2 °C to − 1.4 °C.

Small patches of vegetation seem to have less effect on decreasing the temperature even when there is a high number compared to larger green areas. This was also observed by Liu et al. (2022) in Shijiazhuang (China). They concluded that larger patches of vegetation leading to a less fragmented landscape tend to reduce LST. This contrasts with a study performed in Adelaide (Australia) (Ossola et al., 2021) which showed that even though small patches of vegetation did not affect LST at city scale using a 2 m ground resolution, they decreased local LST by up to 6 ℃ during the day. This effect largely depended, however, on their location within the urban area.

Furthermore, the state of the vegetation and the environmental conditions are important. For example, the cooling provided by vegetation in dry climates can be reduced by limited evapotranspiration (Manoli et al., 2020) if adequate irrigation is not provided.

4.1. Limitations of the study

The fact that the results obtained applying this methodology rely on the satellite images selected by the user and fed to the system constitutes its main drawback. The final result might be affected if this selection is inadequate, or there is missing or incorrect information in many pixels (e.g., due to clouds). This selection will also affect the map with the unfavourable zones as the user can also determine which areas will be included in the analysis within a particular city. For example, if the user decides to exclude industrial areas, the DAI values might change in other parts of the city.

Taking into account the dates of the satellite images used for the analysis is important. Only images during the summer were considered in our study, when the most unfavourable situation is expected. Obviously, the results will be different if images taken during other seasons of the year are used, which can also affect the visualization of the DAI

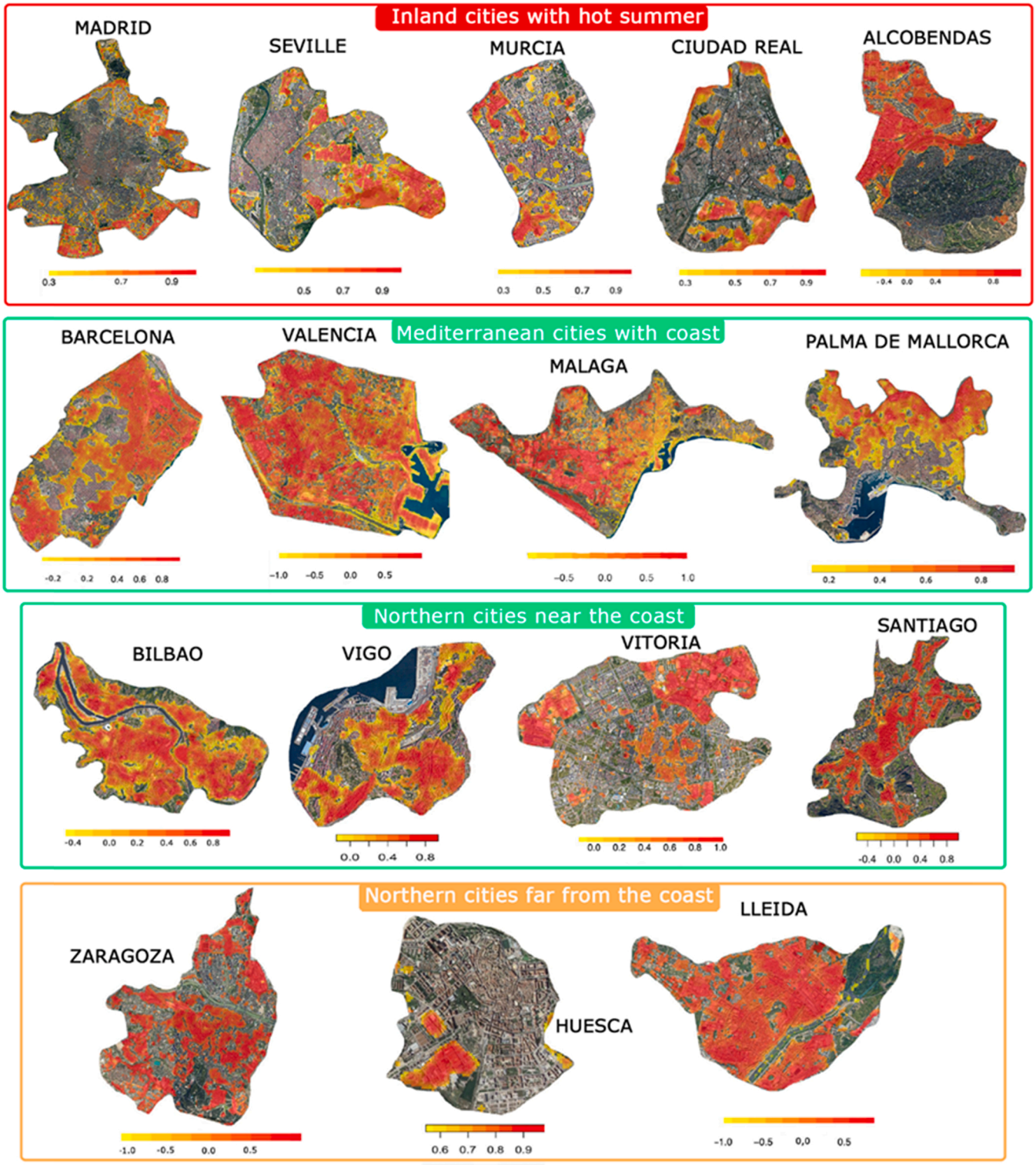

Fig. 2. The most unfavourable areas are depicted in the aerial photograph of each of the cities studied. A reddish colour indicates more disadvantaged zones.

maps. For instance, areas labelled as unfavourable in a DAI map obtained from images captured in summer can appear with vegetation in an aerial view of a city in winter. This happens because they are completely dry and without living vegetation in summer but have a natural green cover in winter.

As an example, Appendix C shows the spatial distribution of land surface temperatures (LST), Normalized Difference Vegetation Index (NDVI), and unfavourable areas with the Disadvantaged Area Index (DAI) values for Seville and Malaga in the different seasons of 2020. Obviously, the LST maps totally differ in the different seasons, but the NDVI maps also change, showing higher NDVI values in more zones in winter and spring, which influences the location and number of unfavourable areas. This is common in cities with mild winters, such as Seville or Malaga, where there are few frost events and the vegetation does not stop growing in this season. Also, the number of perennial species used in public gardening is greater than that of deciduous species. In addition,

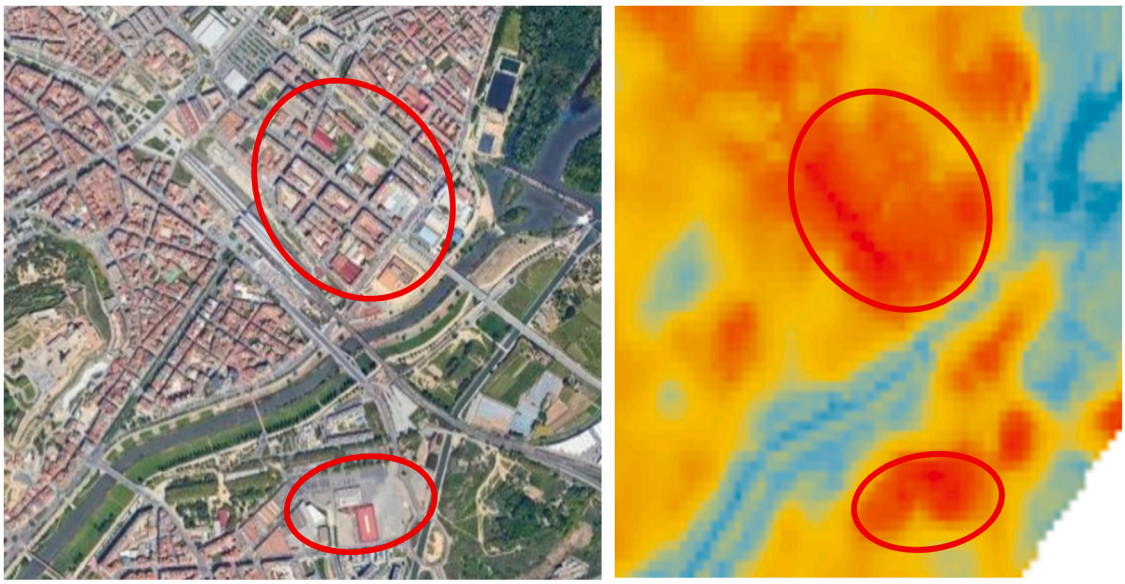

Fig. 3. Aerial photograph of a region of Lleida including two of the most unfavourable areas circled in red (left) and the corresponding thermal image showing high temperatures in red and low in blue (right).

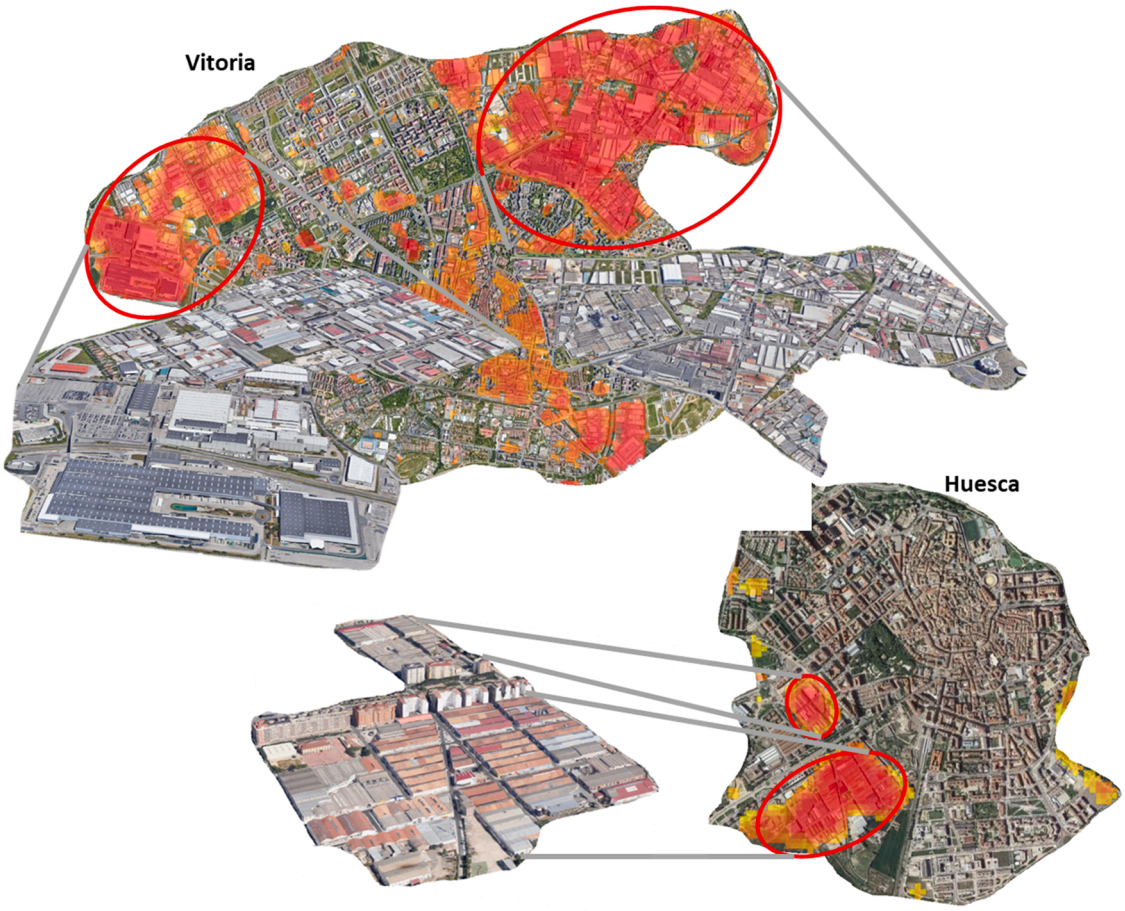

Fig. 4. Details of the industrial areas catalogued as unfavourable in Vitoria (top) and Huesca (bottom).

as there is more humidity in winter, many vacant lots are covered with natural grass, while in summer they hardly have any vegetation. This can be easily observed in the south-eastern part of Seville, where areas with high DAI (labelled as unfavourable) in summer and autumn, have low DAI in winter and spring (mainly due to higher NDVI values).

The number of images considered to study the situation in a certain city is also important. Several images should be employed to make good use of the tool for urban planning, as a too low number of images could lead to unrepresentative results. However, though different seasons can be analysed, it is advisable to use images corresponding to the most

unfavourable situations (that is, higher temperatures, usually in summer).

In addition, the time of acquisition of the image is conditioned to the hour when the satellite is over a certain city. For that reason, evaluating the effect of UGI on LST during the evening or at night was not possible in our case. Images from other satellites passing at the desired time should have been used.

The resolution of the images acquired by the satellite also greatly influences the results. For example, in our study, the NDVI values were usually not high, barely exceeding 0.6 (dense vegetation category). This can be explained due to the use of Landsat 30x30m images, given that it is difficult for a complete pixel of 900 m^2 to be full of vegetation, and it frequently includes some areas without plants that lower the average NDVI of the pixel. As an example, Farina (2012) also reported low NDVI values with an average of 0.36 for green urban areas of Seville, using data acquired by Landsat 7. Some NDVI values would be higher in smaller pixels for images acquired by other satellites with higher resolution (e.g., Sentinel, Worldview) or aerial platforms (e.g., UAV), as shown by other authors in Seville (Herrera-Gomez et al., 2017) or in other locations (Nouri et al., 2014). This will affect the precision of the classification of the different areas (Labib and Harris, 2018). At the same time, the effects of UGI in LST will be less appreciated when using low resolution images (Liu et al., 2022).

Precisely due to these issues with the resolution or the time of acquisition of the image, using vegetation indexes such as NDVI can be problematic in order to accurately quantify the vegetation present in an area. Therefore, combining these indexes with other methods such as ground truth collection, machine learning from aerial RGB images, or LIDAR can improve the results (Lafortezza and Giannico, 2019).

In any case, in order to validate the identification of vegetated areas according to NDVI values performed in our study, we compared the green areas detected in two of the cities (Malaga and Seville) with the Land Cover/Use classes established in the Urban Atlas Copernicus project (Appendix D). As observed, the level of coincidence between the identified green areas and the land uses corresponding to the existence of vegetation is high. In both cities used as examples, there are additional areas catalogued as green that are not within the land uses considered. However, in most cases, they correspond to zones with many street trees or locations devoted to sport facilities (such as golf courses) or urban agriculture.

The methodology used serves as a tool to consider which areas are more in need of including green spaces. Within the resulting unfavourable zones, other factors should be considered, such as space availability, land use, or existing constructions (and the feasibility of integrating vegetation on them).

5. Conclusions

A methodology was developed for the use of satellite images to identify which parts of a city are in greater need of vegetation due to excessive temperatures and lack of green spaces. It was applied to sixteen Spanish cities with different characteristics where the most unfavourable areas were determined and showed on a map. The calculation of the Disadvantaged Area Index offers an indicator that allows the degree of unfavorability to be defined.

In a context of limited resources to increase vegetation in cities, detecting unfavourable areas constitutes a very interesting tool for public administrations, municipal policy makers and urban planners to define the future planning strategy for green spaces in order to decide which locations should be prioritised to be vegetated in a city. In this sense, the usefulness of the information provided by the DAI map is clear, since it allows those that are really much more unfavourable, within the critical areas, to be detected.

CRediT authorship contribution statement

Francisco Rodríguez-Gómez: Methodology, Software, Validation, Resources, Data curation, Writing – original draft, Writing – review & editing, Visualization. **Rafael Fernández-Cañero:** Conceptualization, Validation, Resources, Writing – review & editing. **Gabriel Pérez:** Validation, Resources, Writing – review & editing. **José del Campo-Ávila:** Software, Writing – review & editing. **Domingo López-Rodríguez:** Software, Validation, Formal analysis, Writing – review & editing. **Luis Pérez-Urrestarazu:** Conceptualization, Methodology, Validation, Resources, Writing – original draft, Writing – review & editing, Visualization, Supervision, Funding acquisition.

Declaration of Competing Interest

The authors declare the following financial interests/personal relationships which may be considered as potential competing interests: Luis Perez-Urrestarazu reports financial support was provided by Spanish Ministry of Science, Innovation and Universities.

Acknowledgements

This study was financed by the Spanish R & D Programme for projects addressing the challenges of the society (2018 call), in the framework of the State Plan of Scientific and Technical Research and Innovation 2017–2020, financed by the Spanish Ministry of Science, Innovation and Universities, grant number RTI2018095097-B-100.

Appendix A. Supporting information

Supplementary data associated with this article can be found in the online version at doi:10.1016/j.ufug.2022.127783.

References

AEMET, n.d. Resúmenes climatológicos - C. Autónomas - Agencia Estatal de Meteorología - AEMET. Gobierno de España [WWW Document]. URL ⟨http://www.aemet.es/es/serviciosclimaticos/vigilancia_clima/resumenes?w=1⟩ (Accessed 2.14.22).

Aletba, S.R.O., Abdul Hassan, N., Putra Jaya, R., Aminudin, E., Mahmud, M.Z.H., Mohamed, A., Hussein, A.A., 2021. Thermal performance of cooling strategies for asphalt pavement: a state-of-the-art review. J. Traffic Transp. Eng. (Engl. Ed.) 8, 356–373. https://doi.org/10.1016/J.JTTE.2021.02.001.

Cai, Z., Han, G., Chen, M., 2018. Do water bodies play an important role in the relationship between urban form and land surface temperature? Sustain Cities Soc. 39, 487–498. https://doi.org/10.1016/J.SCS.2018.02.033.

Chen, A., Yao, X.A., Sun, R., Chen, L., 2014. Effect of urban green patterns on surface urban cool islands and its seasonal variations. Urban For. Urban Green. 13, 646–654. https://doi.org/10.1016/J.UFUG.2014.07.006.

Chen, X.L., Zhao, H.M., Li, P.X., Yin, Z.Y., 2006. Remote sensing image-based analysis of the relationship between urban heat island and land use/cover changes. Remote Sens. Environ. 104, 133–146. https://doi.org/10.1016/j.rse.2005.11.016.

Código Técnico de la Edificación [WWW Document], 2020. URL ⟨https://www.codigotecnico.org/⟩ (Accessed 2.14.22).

Du, H., Cai, W., Xu, Y., Wang, Z., Wang, Y., Cai, Y., 2017. Quantifying the cool island effects of urban green spaces using remote sensing Data. Urban For. Urban Green. 27, 24–31. https://doi.org/10.1016/J.UFUG.2017.06.008.

Environmental Protection Agency, 2014. What is Open Space/Green Space? [WWW Document]. URL ⟨https://www3.epa.gov/region1/eco/uep/openspace.html⟩ (Accessed 8.27.21).

Estoque, R.C., Murayama, Y., Myint, S.W., 2017. Effects of landscape composition and pattern on land surface temperature: An urban heat island study in the megacities of Southeast Asia. Sci. Total Environ. 577, 349–359. https://doi.org/10.1016/j.scitotenv.2016.10.195.

European Commission, 2014. Copernicus [WWW Document]. URL ⟨https://www.copernicus.eu⟩ (accessed 8.27.21).

Farina, A., 2012. Exploring the Relationship Between Land Surface Temperature And Vegetation Abundance For Urban Heat Island Mitigation in Seville, Spain (LUMA-GIS Thesis nr). Lund University, Sölvegatan.

Fusami, A.A., Nweze, O.C., Hassan, R., 2020. Comparing the effect of deforestation result by NDVI and SAVI. Int. J. Sci. Res. Publ. (IJSRP 10, 918–925. https://doi.org/10.29322/IJSRP.10.06.2020.P102110.

Giannico, V., Spano, G., Elia, M., D'Este, M., Sanesi, G., Lafortezza, R., 2021. Green spaces, quality of life, and citizen perception in European cities. Environ. Res. 196, 110922 https://doi.org/10.1016/J.ENVRES.2021.110922.

Grafius, D.R., Edmondson, J.L., Norton, B.A., Clark, R., Mears, M., Leake, J.R., Corstanje, R., Harris, J.A., Warren, P.H., 2020. Estimating food production in an urban landscape. Sci. Rep. 2020 10:1 10, 1–9. https://doi.org/10.1038/s41598-020-62126-4.

Grunewald, K., Richter, B., Meinel, G., Herold, H., Syrbe, R.-U., 2017. Proposal of indicators regarding the provision and accessibility of green spaces for assessing the ecosystem service "recreation in the city" in Germany. https://doi.org/10.1080/21513732.2017.1283361 13, 26–39. ⟨https://doi.org/10.1080/21513732.2017.1283361⟩.

Gupta, K., Kumar, P., Pathan, S.K., Sharma, K.P., 2012. Urban neighborhood green index – a measure of green spaces in urban areas. Land. Urban Plan 105, 325–335. https://doi.org/10.1016/J.LANDURBPLAN.2012.01.003.

Hashim, H., Latif, Z.A., Adnan, N.A., Alam, S., 2019. Urban vegetation classification with NDVI threshold value method with very high resolution (VHR) pleiades imagery, in: 6th International Conference on Geomatics and Geospatial Technology. Kuala Lumpur, Malaysia, pp. 237–240. ⟨https://doi.org/10.5194/isprs-archives-XLII-4-W16–237-2019⟩.

Hathway, E.A., Sharples, S., 2012. The interaction of rivers and urban form in mitigating the Urban Heat Island effect: a UK case study. Build. Environ. 58, 14–22. https://doi.org/10.1016/J.BUILDENV.2012.06.013.

Herrera-Gomez, S.S., Quevedo-Nolasco, A., Pérez-Urrestarazu, L., 2017. The role of green roofs in climate change mitigation. A case study in Seville (Spain). Build. Environ. 123, 575–584.

Holidu, 2019. Estas son las 38 ciudades con más zonas verdes de España [WWW Document]. URL ⟨https://as.com/deporteyvida/2019/05/07/portada/1557226775_767652.html⟩ (Accessed 2.14.22).

Huang, C., Ye, X., 2015. Spatial modeling of urban vegetation and land surface temperature: a case study of Beijing. Sustainability 7, 9478–9504. https://doi.org/10.3390/su7079478.

Imhoff, M.L., Zhang, P., Wolfe, R.E., Bounoua, L., 2010. Remote sensing of the urban heat island effect across biomes in the continental USA. Remote Sens. Environ. 114, 504–513. https://doi.org/10.1016/J.RSE.2009.10.008.

Labib, S.M., Harris, A., 2018. The potentials of Sentinel-2 and LandSat-8 data in green infrastructure extraction, using object based image analysis (OBIA) method. Eur. J. Remote Sens. 51, 231–240. https://doi.org/10.1080/22797254.2017.1419441.

Lafortezza, R., Giannico, V., 2019. Combining high-resolution images and LiDAR data to model ecosystem services perception in compact urban systems. Ecol. Indic. 96, 87–98. https://doi.org/10.1016/J.ECOLIND.2017.05.014.

Levent, T.B., Nijkamp, P., 2017. Evaluation of urban green spaces 1. In: Beyond Benefit Cost Analysis: Accounting for Non-Market Values in Planning Evaluation. Routledge, pp. 63–87. https://doi.org/10.4324/9781351162685-5.

Li, X., Stringer, L.C., Dallimer, M., 2022. The role of blue green infrastructure in the urban thermal environment across seasons and local climate zones in East Africa. Sustain Cities Soc. 80, 103798 https://doi.org/10.1016/J.SCS.2022.103798.

Liao, L., Zhang, L., Bengtsson, L., 2005. Analyzing Dynamic Change of Vegetation Cover of Desert Oasis Based on Remote Sensing Data in Hexi Region, in: Proceedings of the International Symposium on Sustainable Water Resources Management and Oasis-Hydrosphere-Desert Interaction in Arid Regions. Beijing, PR China, pp. 279–295.

Lin, W., Yu, T., Chang, X., Wu, W., Zhang, Y., 2015. Calculating cooling extents of green parks using remote sensing: Method and test. Land. Urban Plan 134, 66–75. https://doi.org/10.1016/J.LANDURBPLAN.2014.10.012.

Liu, K., Li, X., Wang, S., Gao, X., 2022. Assessing the effects of urban green landscape on urban thermal environment dynamic in a semiarid city by integrated use of airborne data, satellite imagery and land surface model. Int. J. Appl. Earth Obs. Geoinf. 107, 102674 https://doi.org/10.1016/J.JAG.2021.102674.

Liu, O.Y., Russo, A., 2021. Assessing the contribution of urban green spaces in green infrastructure strategy planning for urban ecosystem conditions and services. Sustain Cities Soc. 68, 102772 https://doi.org/10.1016/J.SCS.2021.102772.

Manoli, G., Fatichi, S., Bou-Zeid, E., Katul, G.G., 2020. Seasonal hysteresis of surface urban heat islands. Proc. Natl. Acad. Sci. USA 117, 7082–7089. https://doi.org/10.1073/PNAS.1917554117/-/DCSUPPLEMENTAL.

Marzban, F., Sodoudi, S., Preusker, R., 2018. The influence of land-cover type on the relationship between NDVI–LST and LST-Tair. Int. J. Remote Sens 39, 1377–1398. https://doi.org/10.1080/01431161.2017.1402386.

Masoudi, M., Tan, P.Y., 2019. Multi-year comparison of the effects of spatial pattern of urban green spaces on urban land surface temperature. Land. Urban Plan 184, 44–58. https://doi.org/10.1016/J.LANDURBPLAN.2018.10.023.

Mejbel Salih, M., Zakariya Jasim, O., Hassoon, I., Jameel Abdalkadhum, A, K., 2018. Land surface temperature retrieval from LANDSAT-8 thermal infrared sensor data and validation with infrared thermometer camera. Int. J. Eng. Technol. 7, 608. https://doi.org/10.14419/ijet.v7i4.20.27402.

NASA, 1972. Landsat [WWW Document]. URL ⟨https://landsat.gsfc.nasa.gov/⟩ (Accessed 8.27.21).

Nouri, H., Beecham, S., Anderson, S., Nagler, P., 2014. High spatial resolution worldView-2 imagery for mapping NDVI and its relationship to temporal urban landscape evapotranspiration factors. Remote Sens. 6, 580–602. https://doi.org/10.3390/rs6010580.

Ossola, A., Jenerette, G.D., McGrath, A., Chow, W., Hughes, L., Leishman, M.R., 2021. Small vegetated patches greatly reduce urban surface temperature during a summer heatwave in Adelaide, Australia. Land. Urban Plan 209, 104046. https://doi.org/10.1016/J.LANDURBPLAN.2021.104046.

Park, J., Kim, J.-H., Lee, D.K., Park, C.Y., Jeong, S.G., 2017. The influence of small green space type and structure at the street level on urban heat island mitigation. Urban For. Urban Green. 21, 203–212. https://doi.org/10.1016/J.UFUG.2016.12.005.

Qiu, G. yu, Li, H. yong, Zhang, Q. tao, Chen, W., Liang, X. jian, Li, X. ze, 2013. Effects of evapotranspiration on mitigation of urban temperature by vegetation and urban agriculture. J. Integr. Agric. 12, 1307–1315. https://doi.org/10.1016/S2095-3119(13)60543-2.

R Core Team, 2021. R: A language and environment for statistical computing.

Reis, C., Lopes, A., 2019. Evaluating the cooling potential of urban green spaces to tackle urban climate change in Lisbon. Sustainable) 11. https://doi.org/10.3390/su11092480.

Santamouris, M., 2013. Using cool pavements as a mitigation strategy to fight urban heat island—A review of the actual developments. Renew. Sustain. Energy Rev. 26, 224–240. https://doi.org/10.1016/J.RSER.2013.05.047.

Santamouris, M., Paraponiaris, K., Mihalakakou, G., 2007. Estimating the ecological footprint of the heat island effect over Athens, Greece. Clim. Change 80, 265–276. https://doi.org/10.1007/S10584-006-9128-0, 80:3.

Schwaab, J., Meier, R., Mussetti, G., Seneviratne, S., Bürgi, C., Davin, E.L., 2021. The role of urban trees in reducing land surface temperatures in European cities. Nat. Commun. 2021 12:1 12, 1–11. https://doi.org/10.1038/s41467-021-26768-w.

Schwarz, N., Schlink, U., Franck, U., Großmann, K., 2012. Relationship of land surface and air temperatures and its implications for quantifying urban heat island indicators—An application for the city of Leipzig (Germany). Ecol. Indic. 18, 693–704. https://doi.org/10.1016/J.ECOLIND.2012.01.001.

Shahtahmassebi, A.R., Li, C., Fan, Y., Wu, Y., lin, Y., Gan, M., Wang, K., Malik, A., Blackburn, G.A., 2021. Remote sensing of urban green spaces: a review. Urban For. Urban Green. 57, 126946 https://doi.org/10.1016/J.UFUG.2020.126946.

Small, C., 2010. Estimation of urban vegetation abundance by spectral mixture analysis. Int. J. Remote Sens 22, 1305–1334. https://doi.org/10.1080/01431160151144369.

Su, Y., Wu, J., Zhang, C., Wu, X., Li, Q., Liu, L., Bi, C., Zhang, H., Lafortezza, R., Chen, X., 2022. Estimating the cooling effect magnitude of urban vegetation in different climate zones using multi-source remote sensing. Urban Clim. 43, 101155 https://doi.org/10.1016/J.UCLIM.2022.101155.

Sun, R., Xie, W., Chen, L., 2018. A landscape connectivity model to quantify contributions of heat sources and sinks in urban regions. Land. Urban Plan 178, 43–50. https://doi.org/10.1016/J.LANDURBPLAN.2018.05.015.

Susca, T., Gaffin, S.R., Dell'osso, G.R., 2011. Positive effects of vegetation: urban heat island and green roofs. Environ. Pollut. 159, 2119–2126. https://doi.org/10.1016/j.envpol.2011.03.007.

Takebayashi, H., Moriyama, M., 2007. Surface heat budget on green roof and high reflection roof for mitigation of urban heat island. Build. Environ. 42, 2971–2979. https://doi.org/10.1016/j.buildenv.2006.06.017.

Tan, K.C., Lim, H.S., MatJafri, M.Z., Abdullah, K., 2010. Landsat data to evaluate urban expansion and determine land use/land cover change in Penang Island. Malays. Environ. Earth Sci. 60, 1509–1521.

Taufik, A., Sakinah, S., Ahmad, S., Ahmad, A., 2016. Classification of Landsat 8 satellite data using NDVI thresholds. J. Telecommun. Electron. Comput. Eng. 8, 37–40.

Theeuwes, N.E., Steeneveld, G.-J., Ronda, R.J., Holtslag, A.A.M., 2017. A diagnostic equation for the daily maximum urban heat island effect for cities in northwestern Europe. Int. J. Climatol. 37, 443–454. https://doi.org/10.1002/JOC.4717.

Tran, H., Uchihama, D., Ochi, S., Yasuoka, Y., 2006. Assessment with satellite data of the urban heat island effects in Asian mega cities. Int. J. Appl. Earth Obs. Geoinf. 8, 34–48. https://doi.org/10.1016/J.JAG.2005.05.003.

Voogt, J.A., Oke, T.R., 2003. Thermal remote sensing of urban climates. Remote Sens. Environ. 86, 370–384. https://doi.org/10.1016/S0034-4257(03)00079-8.

Wang, R., Zhao, J., Meitner, M.J., Hu, Y., Xu, X., 2019. Characteristics of urban green spaces in relation to aesthetic preference and stress recovery. Urban For. Urban Green. 41, 6–13. https://doi.org/10.1016/J.UFUG.2019.03.005.

Wolch, J.R., Byrne, J., Newell, J.P., 2014. Urban green space, public health, and environmental justice: The challenge of making cities 'just green enough. Land. Urban Plan 125, 234–244. https://doi.org/10.1016/J.LANDURBPLAN.2014.01.017.

Xue, J., Su, B., 2017. Significant remote sensing vegetation indices: a review of developments and applications. J. Sens 2017. https://doi.org/10.1155/2017/1353691.

Yang, C., He, X., Wang, R., Yan, F., Yu, L., Bu, K., Yang, J., Chang, L., Zhang, S., 2017. The effect of urban green spaces on the urban thermal environment and its seasonal variations. Forests 8, 1–19. https://doi.org/10.3390/f8050153.

Yang, L., Zhang, L., Li, Y., Wu, S., 2015. Water-related ecosystem services provided by urban green space: a case study in Yixing City (China). Land. Urban Plan 136, 40–51. https://doi.org/10.1016/J.LANDURBPLAN.2014.11.016.

Yue, W., Xu, J., Tan, W., Xu, L., 2007. The relationship between land surface temperature and NDVI with remote sensing: Application to Shanghai Landsat 7 ETM+ data. Int. J. Remote Sens. 28, 3205–3226. https://doi.org/10.1080/01431160500306906.

Zhu, Z., Wulder, M.A., Roy, D.P., Woodcock, C.E., Hansen, M.C., Radeloff, V.C., Healey, S.P., Schaaf, C., Hostert, P., Strobl, P., Pekel, J.F., Lymburner, L., Pahlevan, N., Scambos, T.A., 2019. Benefits of the free and open landsat data policy. Remote Sens. Environ. 224, 382–385. https://doi.org/10.1016/J.RSE.2019.02.016.